BALNEO RESEARCH JOURNAL
English Edition
eISSN 2069-7619 pISSN 2069-7597 ROMANIAN ASSOCIATION OF BALNEOLOGY

# Perspectives on the use of electrostimulation with the device "VEB"® in the management of disorders related to COVID-19

**Valeriy Ye. Babelyuk[1,2], Igor L. Popovych[2,3], Nazariy V. Babelyuk[1,2], Tetyana A. Korolyshyn[1,3], Galyna I. Dubkova[1], Marta M. Kovbasnyuk[3], Victor Y. Hubyts'kyi[1], Volodymyr V. Kikhtan[1], Vira Y. Musiyenko[1], Iryna G. Kyrylenko[2], Yuriy G. Dobrovolsky[4], Igor H. Korsunskyi[4], Radosław Muszkieta[5], Walery Zukow[5], Anatoliy I. Gozhenko[2]**

Corresponding author: **Walery Zukow**, E-mail: w.zukow@wp.pl

Balneo Research Journal DOI: http://dx.doi.org/10.12680/balneo.2020.361 Vol.11, No.3, September 2020 p: 328–343

1. Clinical Sanatorium "Moldova", Truskavets', Ukraine
2. State Enterprise Ukrainian Research Institute for Medicine of Transport, Ministry of Health of Ukraine, Odesa, Ukraine
3. Bohomolets' Institute of Physiology of NAS, Kyïv, Ukraine
4. Yu Fedkovych Chernivtsi National University, Chernivtsi, Ukraine
5. Nicolaus Copernicus University, Torun, Poland

## Abstract

Background. One of the symptoms of COVID-19 is the so-called "cytokine storm". Its pathogenesis is that the initial release by lymphocytes and macrophages of proinflammatory cytokines in the classical immune response to SARS-CoV-2 is significantly enhanced and maintained due to excessive adrenergic stimulation of the immune cells. The proinflammatory adrenergic mechanism of the "cytokine storm" can be offset by the activation of the anti-inflammatory cholinergic mechanism by non-invasive stimulation of the vagus nerve. In 2015, a generator for electrotherapy and stimulation oh human nerve centers was created, called "VEB-1"®. Preliminary observation of volunteers revealed a modulating effect of a four-day course of electrical stimulation on the parameters of electroencephalogram, metabolism, as well as gas-discharge visualization (GDV). We hypothesized that changes in EEG parameters may be accompanied by a vagotonic shift of the sympatho-vagus balance, favorable for calming the "cytokine storm". The main purpose of this study was to find out. In addition, concomitant changes in EEG, immunity, GDV, etc. due to the use of the devices "VEB-1"® and recently designed "VEB-2" had to be detected. Material and research methods. The object of observation were 18 volunteers: 11 women 33-62 y and 7 men 29-62 y (Mean±SD: 51±12 y) without clinical diagnose but with dysfunction of neuro-endocrine-immune complex and metabolism. In the morning registered HRV ("CardioLab+HRV", "KhAI-Medica", Kharkiv, UA), EEG ("NeuroCom Standard", "KhAI-Medica", Kharkiv, UA), kirlianogram by the method of GDV ("GDV Chamber", "Biotechprogress", SPb, RF), electroconductivity of skin in three pairs of points of acupuncture ("Medissa"), electrokinetic index of buccal epithelium ("Biotest", Kharkiv State University), as well as some parameters of immunity and metabolism. After the initial testing, an electrical stimulation session was performed with a "VEB-1"® or a "VEB-2" devices. The next morning after completing the four-day course, retesting was performed. Results. The effects of electrical stimulation can be divided into the following networks. Regarding EEG, this is a leveling of right-hand lateralization and normalizing decrease in the increased of the amplitude of the θ-rhythm and its spectral power density (SPD) at the loci F3, F7, F8, T3, T4, T6, P3, O1 and O2; further increase of SPD of δ-rhythm in loci F3, F4, T6, P3 and O1 as well as further decrease of SPD F4-α; reversion of the increased level of entropy in loci Fp1, F4, C3 and P3 to the lowered level. Regarding HRV, it is a vagotonic shift of sympatho-vagus balance due to a decrease in elevated levels of sympathetic tone markers and an increase in decreased levels of vagus tone markers, but without normalization. Neurotropic effects are accompanied by favorable changes in a number of immune parameters and a tendency to decrease the level of C-Reactive Protein. Regarding GDV, it is almost complete normalization of the initially increased GDI Area in the frontal projection and third Chakra Energy; normalizing decrease in the initially increased Energy of second and seventh Chakras; normalizing right-hand shift of more or less pronounced left-sided Asymmetry of first and third Chakra. These effects should be clearly interpreted as physiologically beneficial. The effects on these parameters are almost equally pronounced in people of both sexes when using both devices. Conclusion. Vagotonic and immunotropic effects of our device give us a reason to offer it for further research on the leveling of "cytokine storm" in patients with COVID-19.

**Key words:** *electrostimulation, EEG, cytokine cascade, COVID-19, SARS-CoV-2, ACE2 receptors,*

## Introduction

One of the symptoms of COVID-19 is the so-called "cytokine storm". Its pathogenesis is that the initial release by lymphocytes and macrophages of proinflammatory cytokines in the classical immune response to SARS-CoV-2 contact with ACE2 receptors of the nasal mucosa, pharynx, conjunctiva, etc. is significantly enhanced and maintained due to excessive adrenergic stimulation of the immune cells, in turn, caused by the direct effect of SARS-CoV-2 on the sympathetic nuclei of the brain, where it penetrates through the afferent fibers of the vagus and olfactory nerves [Baptista AF et al, 2020].

The proinflammatory adrenergic mechanism of the "cytokine storm" can be offset by the activation of the anti-inflammatory cholinergic mechanism [Borovikova LV et al, 2000; Tracey KJ, 2007,2010; Chavan SS et al, 2017,2017a; Pavlov VA et al, 2018] by non-invasive vagus nerve stimulation (VNS). Direct VNS is realized by electrical stimulation of the nerve endings of the skin through procedures of transcutaneous auricular vagus nerve stimulation (taVNS) or cervical vagus nerve stimulation (nVNS). Indirect VNS is realized by electrical stimulation of the scalp in the locus F3, which is projected left dorsolateral prefrontal cortex, the neurons of which, in turn, activate the nuclei of the vagus [Baptista AF et al, 2020; Bikson M et al, 2020; Fudium M et al, 2020; Staats P et al, 2020; Tornero C et al, 2020]. Hyoju SK et al [2020] offer to achieve the same goal to dampen the sympathetic influences on immune response.

In 2015, a generator for electrotherapy and stimulation oh human nerve centers was created (Babelyuk VE, Dobrovolsky YG, Korsunskyi IH), called “VEB-1”®. Conceiving and creating our device, we were based on the following provisions.

The influence of impulses of a rectangular shape (range 7-18 Hz) made it possible to fix the frequency ranges of each basic nerve node. Low frequency had minimal effects of stimulation on the corresponding nerve node, while high frequency - the maximum. For the effective excitation of nerve centers, the frequency beat method is used. It consists in obtaining oscillations with close frequencies. To obtain the effect of the frequency beats are generated by pulses of rectangular shape to two signal channels. The channels differ in frequency, which is the beat frequency. For example, for obtaining a beat frequency 6 Hz, forming pulses in a first channel to a carrier frequency of 30 Hz, a second channel at a frequency of 36 Hz. When the first pulse is formed on both channels with a phase shift of 0o, we obtain an absolute zero current in the output (Figure 1).

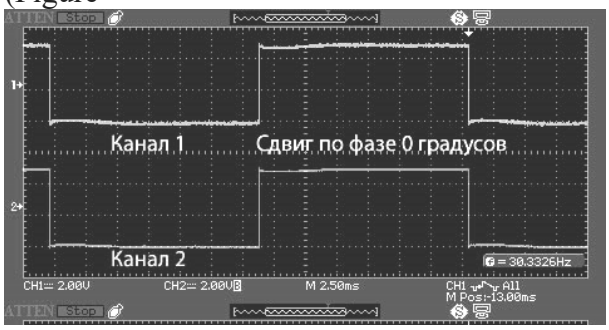


Fig. 1. Oscillogram of the first clock pulse

Figure 2 shows a periodic signal generated by frequency beats voltage in the two channels to form a common output signal (a). Also in Figure 2 is a graph of the current of the output signal (б). Such effect creates a shock wave through the object at the desired frequency. He also spins an electromagnetic field in the object.

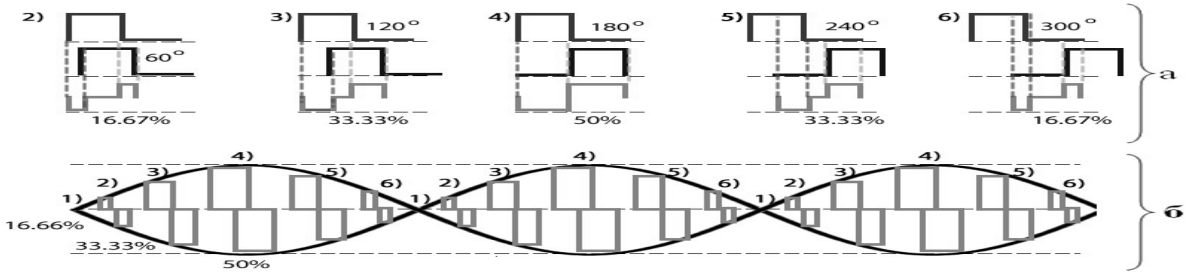


**Fig. 2. Received by frequency beats a periodic signal (a) and a current diagram of the generated output signal (б)**

The generator is assembled on the basis of the patent of Ukraine for utility model 105875 “Portable device for electrotherapy and stimulation” [Babeluk VE, 2016]. Its operation is described in [Babeluk VY et al, 2017].

The generator is assembled on the basis of a two-channel circuit using two frequency synthesizers, amplifiers, each of which generates its own frequency.

Figure 3 shows a block diagram of the device indicating the movement of electric current.

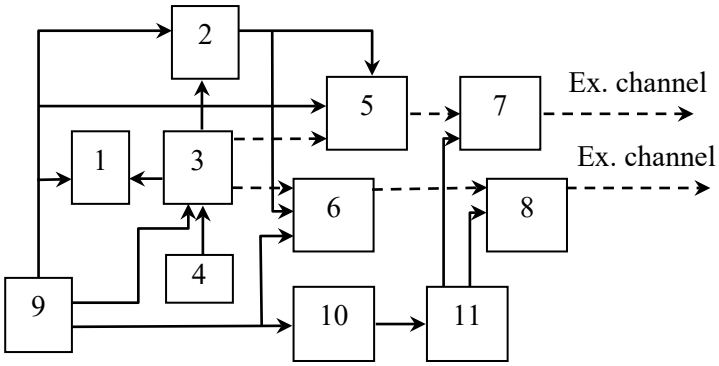


**Fig. 3. A block diagram of the generator VEB-1**

1 - display; 2 - synthesizer of the signal with a sampling frequency up to 0,001 Hz; 3 - micro-controller; 4 - the encoder; 5 - channel A signal synthesizer; 6 - synthesizer of the channel B signal; 7 - channel A signal amplifier; 8 - the amplifier of a signal of the channel B; 9 - battery 5 V; 10 - voltage converter 5-24 V; 11 - voltage regulator; 12 - amplitude control of the output signal.

**Table 1. The technical characteristics of the generator**

| Parameter | Parameter norm |
|---|---|
| The maximum power consumption, W | 1,2 |
| Output signal level by amplitude, V | 3,6-16,2 |
| The maximum amplitude of the output signal, V | 16,2 |
| The maximum possible current impact mA | 25 |
| Ripping protection when current exceeds 25 mA | yes |
| Operating current, mA | 8-18 |
| The shape of the output signal | Meander |
| Frequency range of action, Hz | 144-1120 |
| Power battery voltage, V | 4,8-5,3 |
| Continuous operation time, hours | 8 |

Transmission of the electrical signal to the patient is carried out by means of contact copper electrodes through the wires. The generator operates as follows. Instrument software sets the operating frequency of the pulse beats 0,01-100 Hz with steps on each channel is not more than 0,001 Hz. Discreteness in each channel is not more than 0,001 Hz is provided by a clock synthesizer (2). It forms the frequency corresponding to the number of filling of the thirty two-bit synthesizer frequency (5,6) divided by 1000.

The appearance of the generator with a set of necessary equipment is shown in Figure 4.


**Fig. 4. The appearance of the generator with a set of necessary equipment**

1 - generator VEB-1; 2 - two cords with JACK connectors and terminal clamps for connection to OUT-A and OUT-B outputs; 3 - contact pads or tubes; 4 - power cable with connectors USB-B and USB-A; 5 - battery 5 V.

Preliminary observation of volunteers, among whom was also the authors, revealed a modulating effect of electrical stimulation (during 21 min four days in a row) on the parameters of electroencephalogram (EEG), metabolism, as well as gas-discharge visualization (GDV) [Babelyuk NV et al, 2015,2016,2016a,2018; Babelyuk VYe et al, 2018; Kindzer BM et al, 2019].

Recently designed device "VEB-2". In contrast to the device “VEB-1”, designed to stimulate nerve centers, the electrostimulator “VEB-2” (Fig. 5) implemented an additional channel for input of information impulses into the body - channel C, whose task is the local concentration of the field, which is formed by two signal channels (A and B) to the point and body of the person as close as possible to the organ affected (heart, liver, spleen, right and left kidneys) at frequencies that contribute to the maximum recovery of the organ.

The first part of the program for adjusting the level of the output signal lasts 20 seconds, after which the main part of the program (generation of pulse current of alternating frequency in the range from 144 Hz to 1120 Hz) lasts for 21 ("VEB-1") or 26 ("VEB-2") minutes.

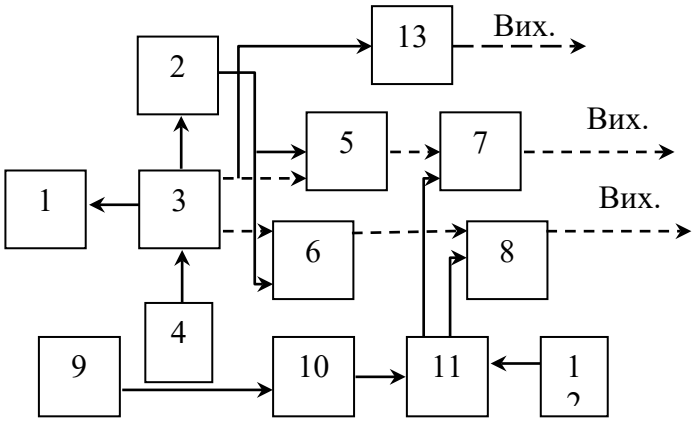


**Fig. 5. A block diagram of the generator VEB-2**
1 - display; 2 - clock signal synthesizer; 3 - controller; 4 - encoder; 5 - signal synthesizer channel A; 6 - signal synthesizer channel B; 7 - signal amplifier channel A; 8 - signal amplifier channel B; 9 - 5 V battery; 10 - voltage converter 5-24 V; 11 - voltage regulator; 12 - regulator of the amplitude of the output signal; 13 - channel filter C

It is known about the functional relationships between EEG and HRV parameters [Ohtake Y et al, 2007; Tang Yi-Y et al, 2009; Tolkunov D et al, 2010; Subhani AR et al, 2012; Prinsloo GE et al, 2013; Popovych IL et al, 2013,2014; Vanneste S, De Ridder D, 2013] as well as neuroimmunomodulation [Korneva EA, 1993; Sternberg EM, 2006; Nance DM, Sanders VM, 2007; Tracey KJ, 2007,2010; Popovych IL, 2008; Thayer JF, Sternberg EM, 2010; Kul'chyns'kyi AB et al, 2017; Popovych IL et al, 2017,2018a,2020; Popadynets' OO et al, 2020]. From here we hypothesized that changes in EEG parameters may be accompanied by a vagotonic shift of the sympatho-vagus balance, favorable for calming the "cytokine storm". The main purpose of this study was to find out. In addition, concomitant changes in EEG, immunity, GDV, etc. due to the use of the devices "VEB-1"® and recently designed "VEB-2" had to be detected.

## MATERIAL AND RESEARCH METHODS

The object of observation were 18 volunteers: 11 women 33-62 y and 7 men 29-62 y (Mean±SD: 51±12 y) without clinical diagnose but with dysfunction of neuro-endocrine-immune complex and metabolism documented previously.

In the morning on an empty stomach registered (**Dubkova GI**) first kirlianogram by the method of GDV by the device of "GDV Chamber" ("Biotechprogress", SPb, RF). Method of GDV, essence of which consists in registration of photoelectronic emission of skin, induced by high-frequency electromagnetic impulses, allows to estimate integrated psycho-somatic state of organism. The first base parameter of GDV is area of gas discharge image (GDI) in Right, Frontal and Left projections registered both with and without polyethylene filter. The second base parameter is a coefficient of shape (ratio of square of length of external contour of GDI toward his area), which characterizes the measure of serration/fractality of external contour. The third base parameter of GDI is entropy, id est measure of chaos. It is considered that GDI, taken off without filter, characterizes the functional changes of organism, and with a filter characterizes organic changes. Program estimates also Energy and Asymmetry of virtual Chakras [Korotkov KG, 2001,2007,2014].

As the attitude to the GDV method is ambiguous, our laboratory conducted studies that proved its relevance [Popovych IL et al, 2010; Babelyuk VY, 2013; Babelyuk VY et al, 2017b,2018].

In addition, the response of GDV parameters to the course of use of bioactive water Naftussya [Gozhenko AI et al, 2016], the course of rehabilitation by Kozyavkin's method [Babelyuk VY et al, 2018a; Popovych IL et al, 2018; Kozyavkina OV et al, 2018,2018a], as well as the immediate response to Katas of Kyokushin Karate operator [Babelyuk VY et al, 2017a] were demonstrated.

Then recorded (**Korolyshyn TA**) simultaneosly electrocardiogram (ECG) and electroencephalogram (EEG). ECG recorded during 7 min in II lead to assess the parameters of heart rate variability (HRV) (hardware-software complex "CardioLab+HRV" production "KhAI-Medica", Kharkiv, Ukraine). For further analysis the following parameters HRV were selected. Temporal parameters (Time Domain

Methods): heart rate (HR), the standart deviation of all NN intervals (SDNN), the square root of the mean of the sum of the squares of differences between adjacent NN intervals (RMSSD), the percent of interval differences of successive NN intervals greater then 50 ms ($pNN_{50}$), triangulary index (TNN). Spectral parameters (Frequency Domain Methods): spectral power density (SPD) bands of HRV: high-frequency (HF, range 0,4÷0,15 Hz), low-frequency (LF, range 0,15÷0,04 Hz), very low-frequency (VLF, range 0,04÷0,015 Hz) and ultra low-frequency (ULF, range 0,015÷0,003 Hz) [HRV,1996; Berntson GG et al, 1997]. Baevskiy's parameters: mode (Mo), the amplitude of mode (AMo), variational sweep (MxDMn) [Baevskiy RM et al, 2001]. We calculated classical indexes: LF/HF, LFnu=100%•LF/(LF+HF), Centralization Index (CI=(VLF+LF)/HF), Baevskiy's Stress Index (BSI=AMo/2•Mo•MxDMn).

EEG recorded during 25 sec a hardware-software complex "NeuroCom Standard" (KhAI Medica, Kharkiv, Ukraine) monopolar in 16 loci (Fp1, Fp2, F3, F4, F7, F8, C3, C4, T3, T4, P3, P4, T5, T6, O1, O2) by 10-20 international system, with the reference electrodes A and Ref on the earlobes. Among the options considered the average EEG amplitude (μV), average frequency (Hz), frequency deviation (Hz), index (%), coefficient of asymmetry (%), absolute ($\mu V^2$/Hz) and relative (%) SPD of basic rhythms: β (35÷13 Hz), α (13÷8 Hz), θ (8÷4 Hz) and δ (4÷0,5 Hz) in all loci, according to the instructions of the device. In addition, calculated Laterality Index (LI) for SPD each Rhythm using formula [Newberg AB et al, 2001]:

LI, % = Σ [200•(Right – Left)/(Right + Left)]/8

We calculated for HRV and each locus EEG the Entropy (h) of normalized SPD using formulas [Popadynets' OO et al, 2019] based on classic Shannon's CE [1963] formula:

$$hHRV=[SPHF•\log_2SPHF+SPLF•\log_2SPLF+SPVLF•\log_2 SPVLF+SPULF•\log_2SPULF]/\log_24$$

$$hEEG = -[SPDα•\log_2SPDα+SPDβ•\log_2SPDβ+SPDθ•\log_2SPDθ+SPDδ•\log_2SPDδ]/\log_24$$

Electroconductivity recorded (**Hubyts'kyi VY**) in follow points of acupuncture: Pg(ND), TR(X) and MC(AVL) at Right and Left side, which represents the nervous, endocrine and immune systems respectively [Hubyts'kyi VY et al, 2013]. Used complex "Medissa". For each pair, the Laterality Index was calculated according to the already mentioned formula.

Parameters of phagocytic function of neutrophils estimated as described by Douglas SD and Quie PG [1981] with our (**Kovbasnyuk MM**) moderately modification. To do this, 5 drops of blood immediately after collection, made in glass centrifuge tubes with 2 ml of 4% solution of sodium citrate. Blood samples were stored in a refrigerator at a temperature of $4^0$C. Further samples were centrifuged (5000 rev/min for 5 min). The supernatant was removed with the help of the Pasteur's pipette. We used a fraction of leukocytes with traces of erythrocytes. The objects of phagocytosis served daily cultures of Staphylococcus aureus (ATCC N 25423 F49) as typical specimen for Gram-positive Bacteria and Escherichia coli (O55 K59) as typical representative of Gram-negative Bacteria. Both cultures obtained from Laboratory of Hydro-Geological Regime-Operational Station JSC "Truskavets'kurort". To prepare the suspension microbes did wipes with relevant shoals sterile saline, immersed tubes in boiling water for 3 seconds, cooled to room temperature. Integrity microbes controlled with the aid of a microscope. To do this, drop the suspension of microbes applied to skimmed substantive piece of glass, fixed in alcohol lamp flame. Ready preparations stained by Papenheim, microscoped during immersion, lense h90, eyepiece x10. The test samples were prepared as follows. In Vidal's plastic tubes made in the following order of 0,05 mL of heparin, 0,05 mL of sterile saline, 0,1 mL suspension of leukocytes, 0,05 mL suspension of microbial bodies. Samples shaked and placed in thermostat at $37^0$C for 30 min, shaking them with every 10 mins. Then, to stop phagocytosis, the sample was cooled under running water for 10 min. In further samples are centrifuged (5000 rev/min, for 5 min), the supernatant removed with the help of the Pasteur's pipette. From the suspension of leukocytes (with traces of red blood cells) prepared strokes, dried in air at room temperature and stained by Papenheim. Microscoped during immersion lens h90, x10 eyepiece. Take into account the following parameters of phagocytosis: activity (percentage of neutrophils, in which found microbes - Hamburger's Phagocytic Index), intensity (number of microbes absorbed one phagocytes - Microbial Count or Right's Index) and completeness (percentage of

dead microbes - Killing Index). Microbial number and index their digestion is determined for each phagocyte and fixed in phagocytic frame.

For phenotyping subpopulations of lymphocytes used the methods of rosette formation with sheep erythrocytes on which adsorbed monoclonal antibodies against receptors CD3, CD4, CD8, CD22 and CD56 from company "Granum" (Kharkiv) with visualization under light microscope with immersion system. Subpopulation of T cells with receptors high affinity determined by test of "active" rosette formation. The state of humoral immunity judged by the concentration in serum of Immunoglobulins classes G, A, M (ELISA, analyser "Immunochem", USA) and circulating immune complexes (by polyethylene glycol precipitation method) [Lapovets' LYe, Lutsyk BD, 2002].

We calculated also the Entropy of Immunocytogram (ICG) and Leukocytogram (LCG) as well as Popovych's Leukocytary Strain Index (PSI-2) using formulas:

$hICG = - [CD4 \bullet \log_2 CD4 + CD8 \bullet \log_2 CD8 + CD22 \bullet \log_2 CD22 + CD56 \bullet \log_2 CD56]/\log_2 4$

$hLCG = - [L \bullet \log_2 L + M \bullet \log_2 M + E \bullet \log_2 E + SNN \bullet \log_2 SNN + StubN \bullet \log_2 StubN]/\log_2 5$

$PSI\text{-}2 = [(Eosinoph/2{,}75\text{-}1)^2 + (StubNeutroph/4{,}25\text{-}1)^2 + (Monoc/6\text{-}1)^2 + (Leukocyt/5\text{-}1)^2]/4$

Then determined (**Musiyenko VY and Kyrylenko IG**) the Electrokinetic Index as rate of electronegative nuclei of buccal epithelium by intracellular microelectrophoresis on the device "Biotest" (Kharkiv State University), according to the method described [Shakhbazov VG, 2000].

At last in portion of venous blood determined (**Kikhtan VV**) plasma level of C-reactive protein (by the ELISA with the use of analyzer "RT-2100C"), total cholesterol (by a direct method after the classic reaction by Zlatkis-Zack) and content of him in composition of high-density lipoproteins (by the enzyme method) according to instructions with the use of analyzers "Reflotron" (BRD) and "Pointe-180" (USA) and corresponding sets of reagents.

Reference values are taken from the database of our laboratory.

Results processed (**Popovych IL**) using the software package "Statistica 8.0".

## RESULTS AND DISCUSSION

Obviously, the presentation of results should begin with changes in EEG parameters. According to the results of screening of direct differences between the values of the parameters after and before electrical stimulation, 41 were found to be significant. Of these, the discriminant analysis program (forward stepwise method) included only 23 in the model, and other parameters (variables) were outside the discriminant model, apparently as carriers of redundant discriminatory information (Tables 1 and 2).

Pseudo-staining gives the visual impression that the most numerous set of EEG parameters that are subject to electrical stimulation are **θ-rhythm** parameters, the other two networks form **δ-rhythm** and **entropy** parameters, while **α-rhythm** is represented by only two parameters, and **β-rhythm** was not subject to significant effects of electrical stimulation.

**Table 1. Discriminant Function Analysis Summary for EEG Variables**

Step 23, N of vars in model: 23; Grouping: Before and After Electrostimulation

Wilks' Lambda: 0,048; approx. $F_{(23,1)}=10{,}4$; $p<10^{-4}$

| | Reference value (122) | Average value | | Wilks' statistics parameters | | | | |
|---|---|---|---|---|---|---|---|---|
| Variables currently in the model | | Before (18) | After (18) | Wilks' Λ | Partial Λ | F-remove | p-level | Tole-rancy |
| θ rhythm Laterality Index, % | -3 | 14 | -4 | 0,197 | 0,243 | 37,32 | $<10^{-4}$ | 0,046 |
| F3-θ SPD, % | 9,6 | 11,5 | 9,7 | 0,203 | 0,237 | 38,66 | $<10^{-4}$ | 0,011 |
| F8-θ SPD, % | 8,4 | 12,5 | 9,0 | 0,068 | 0,701 | 5,11 | 0,043 | 0,071 |
| T3-θ SPD, % | 8,5 | 10,1 | 8,5 | 0,146 | 0,328 | 24,54 | $<10^{-3}$ | 0,026 |
| T6-θ SPD, % | 7,2 | 9,8 | 7,5 | 0,075 | 0,642 | 6,70 | 0,024 | 0,062 |
| F8-θ SPD, $\mu V^2/Hz$ | 19 | 48 | 28 | 0,051 | 0,936 | 0,82 | 0,382 | 0,119 |
| P3-θ SPD, % | 7,8 | 10,3 | 8,4 | 0,052 | 0,914 | 1,12 | 0,310 | 0,100 |
| θ rhythm Amplitude, μV | 7,4 | 10,9 | 9,5 | 0,230 | 0,209 | 45,46 | $<10^{-4}$ | 0,007 |
| O1-θ SPD, % | 6,7 | 10,1 | 8,3 | 0,067 | 0,719 | 4,68 | 0,051 | 0,048 |
| F7-θ SPD, % | 7,9 | 11,5 | 8,9 | 0,056 | 0,860 | 1,95 | 0,188 | 0,061 |
| O2-θ SPD, % | 6,0 | 9,6 | 7,2 | 0,054 | 0,890 | 1,48 | 0,248 | 0,038 |
| T4-θ SPD, % | 8,7 | 10,3 | 8,2 | 0,335 | 0,143 | 71,84 | $<10^{-5}$ | 0,011 |
| Fp1 SPD Entropy | 0,81 | 0,85 | 0,77 | 0,073 | 0,658 | 6,23 | 0,028 | 0,080 |
| C3 SPD Entropy | 0,83 | 0,87 | 0,77 | 0,087 | 0,552 | 9,73 | 0,009 | 0,059 |
| F4 SPD Entropy | 0,82 | 0,85 | 0,76 | 0,072 | 0,671 | 5,89 | 0,032 | 0,026 |
| P3 SPD Entropy | 0,80 | 0,80 | 0,72 | 0,362 | 0,132 | 78,62 | $<10^{-6}$ | 0,016 |
| F3-δ SPD, $\mu V^2/Hz$ | 213 | 222 | 751 | 0,164 | 0,293 | 28,96 | $<10^{-3}$ | 0,008 |
| F4-δ SPD, $\mu V^2/Hz$ | 155 | 183 | 592 | 0,098 | 0,489 | 12,53 | 0,004 | 0,030 |
| T6-δ SPD, % | 30,5 | 35,7 | 45,4 | 0,127 | 0,378 | 19,77 | $<10^{-3}$ | 0,035 |
| T6-δ SPD, $\mu V^2/Hz$ | 276 | 204 | 621 | 0,078 | 0,611 | 7,63 | 0,017 | 0,011 |
| P3-δ SPD, % | 26,5 | 31,2 | 43,0 | 0,141 | 0,341 | 23,21 | $<10^{-3}$ | 0,026 |
| O1-δ SPD, % | 26,7 | 31,8 | 42,0 | 0,232 | 0,207 | 46,04 | $<10^{-4}$ | 0,011 |
| F4-α SPD, % | 32,7 | 25,9 | 22,3 | 0,197 | 0,243 | 37,32 | $<10^{-4}$ | 0,020 |

| Variables currently not in the model | Refer value | Before | After | Wilks' Λ | Partial Λ | F to enter | p-level | Tole-rancy |
|---|---|---|---|---|---|---|---|---|
| C3-θ SPD, % | 9,6 | 12,9 | 9,5 | 0,046 | 0,967 | 0,37 | 0,554 | 0,046 |
| C4-θ SPD, % | 9,7 | 11,9 | 8,9 | 0,044 | 0,926 | 0,88 | 0,369 | 0,044 |
| Fp2-θ SPD, % | 8,3 | 10,7 | 7,6 | 0,047 | 0,981 | 0,21 | 0,658 | 0,047 |
| F4-θ SPD, % | 10,1 | 12,3 | 8,7 | 0,047 | 0,977 | 0,26 | 0,623 | 0,047 |
| F3 SPD Entropy | 0,81 | 0,84 | 0,75 | 0,047 | 0,984 | 0,18 | 0,678 | 0,047 |
| F8 SPD Entropy | 0,75 | 0,81 | 0,73 | 0,046 | 0,966 | 0,38 | 0,549 | 0,046 |
| T3 SPD Entropy | 0,81 | 0,84 | 0,76 | 0,048 | 0,999 | 0,01 | 0,929 | 0,048 |
| C4 SPD Entropy | 0,84 | 0,88 | 0,76 | 0,046 | 0,957 | 0,49 | 0,499 | 0,046 |
| O2 SPD Entropy | 0,73 | 0,81 | 0,75 | 0,048 | 0,996 | 0,04 | 0,840 | 0,042 |
| P4 SPD Entropy | 0,79 | 0,81 | 0,76 | 0,047 | 0,969 | 0,35 | 0,567 | 0,054 |
| Fp2 SPD Entropy | 0,80 | 0,80 | 0,74 | 0,048 | 0,998 | 0,02 | 0,891 | 0,048 |
| C3-δ SPD, % | 29,3 | 22,5 | 44,0 | 0,048 | 0,991 | 0,10 | 0,758 | 0,048 |
| C3-δ SPD, $\mu V^2/Hz$ | 139 | 135 | 351 | 0,047 | 0,980 | 0,23 | 0,641 | 0,047 |
| C4-δ SPD, % | 29,9 | 33,3 | 44,9 | 0,047 | 0,983 | 0,20 | 0,667 | 0,047 |
| F4-δ SPD, % | 32,7 | 36,9 | 47,1 | 0,046 | 0,957 | 0,49 | 0,499 | 0,046 |
| P4-δ SPD, % | 27,1 | 32,7 | 39,7 | 0,048 | 0,998 | 0,02 | 0,896 | 0,058 |
| O2-δ SPD, % | 25,9 | 30,0 | 39,1 | 0,047 | 0,989 | 0,12 | 0,737 | 0,056 |
| F4-α SPD, $\mu V^2/Hz$ | 128 | 64 | 41 | 0,047 | 0,977 | 0,25 | 0,624 | 0,047 |

**Table 2. Summary of Stepwise Analysis for EEG Variables (ranked by criterion Lambda)**

| Variables currently in the model | F to enter | p-level | Lambda | F-value | p-level |
|---|---|---|---|---|---|
| C3 SPD Entropy | 4,72 | 0,037 | 0,878 | 4,72 | 0,037 |
| F8-θ SPD, % | 2,90 | 0,098 | 0,807 | 3,94 | 0,029 |
| F3-θ SPD, % | 2,08 | 0,159 | 0,758 | 3,41 | 0,029 |
| P3 SPD Entropy | 1,59 | 0,217 | 0,721 | 3,00 | 0,033 |
| P3-θ SPD, % | 2,63 | 0,115 | 0,663 | 3,05 | 0,024 |
| θ rhythm Amplitude, μV | 3,78 | 0,062 | 0,586 | 3,41 | 0,011 |
| O1-θ SPD, % | 4,66 | 0,040 | 0,503 | 3,96 | 0,004 |
| F3-δ SPD, $\mu V^2/Hz$ | 1,88 | 0,182 | 0,470 | 3,81 | 0,004 |
| O1-δ SPD, % | 1,79 | 0,193 | 0,440 | 3,68 | 0,004 |
| T4-θ SPD, % | 2,53 | 0,124 | 0,399 | 3,76 | 0,003 |
| F8-θ SPD, $\mu V^2/Hz$ | 2,97 | 0,098 | 0,355 | 3,96 | 0,002 |
| θ rhythm Laterality Index, % | 3,13 | 0,090 | 0,313 | 4,21 | 0,002 |
| T3-θ SPD, % | 2,75 | 0,112 | 0,278 | 4,39 | 0,001 |
| P3-δ SPD, % | 1,73 | 0,202 | 0,257 | 4,34 | 0,001 |
| F4-α SPD, % | 2,17 | 0,156 | 0,232 | 4,42 | 0,001 |
| F4-δ SPD, $\mu V^2/Hz$ | 3,40 | 0,081 | 0,197 | 4,85 | $<10^{-3}$ |
| T6-δ SPD, % | 6,20 | 0,023 | 0,146 | 6,18 | $<10^{-3}$ |
| T6-δ SPD, $\mu V^2/Hz$ | 4,57 | 0,047 | 0,115 | 7,25 | $<10^{-4}$ |
| Fp1 SPD Entropy | 2,34 | 0,146 | 0,101 | 7,53 | $<10^{-4}$ |
| T6-θ SPD, % | 2,43 | 0,140 | 0,087 | 7,92 | $<10^{-4}$ |
| F7-θ SPD, % | 2,49 | 0,137 | 0,073 | 8,41 | $<10^{-4}$ |
| F4 SPD Entropy | 4,72 | 0,049 | 0,054 | 10,4 | $<10^{-4}$ |
| O2-θ SPD, % | 1,48 | 0,248 | 0,048 | 10,3 | $<10^{-4}$ |
| $r^*=0,976$; Wilks' $\Lambda=0,048$; $\chi^2_{(23)}=68,3$; $p<10^{-5}$ | | | | | |
| Squared Mahalanobis Distance=79; F=10; $p<10^{-4}$ | | | | | |

Recognition information is condensed in the canonical discriminant root, which, judging by the Structural coefficients, reflects 17 variables directly and 6 inversely (Table 3). The same table also shows the Raw coefficients, the sum of the products of which on the individual values of discriminant variables together with the Constant gives the individual values of the root before and after the course of electrical stimulation (Fig. 6).

**Table 3. Standardized, Structural and Raw Coefficients and Constant for EEG Variables (ranked by Structural coefficient)**

| | Coefficients | | |
|---|---|---|---|
| Variables currently in the model | Standardized | Structural | Raw |
| C3 SPD Entropy | 2,829 | 0,084 | 20,56 |
| F8-θ SPD, $\mu V^2/Hz$ | 2,109 | 0,075 | 0,385 |
| T6-θ SPD, % | -2,463 | 0,070 | -0,652 |
| P3 SPD Entropy | 7,549 | 0,062 | 47,58 |
| F8-θ SPD, % | 0,753 | 0,061 | 0,020 |
| O2-θ SPD, % | 1,729 | 0,059 | 0,361 |
| F4 SPD Entropy | -3,639 | 0,059 | -20,69 |
| θ rhythm Laterality Index, % | 4,156 | 0,058 | 0,111 |
| Fp1 SPD Entropy | 2,125 | 0,055 | 12,17 |
| F7-θ SPD, % | -1,553 | 0,053 | -0,271 |
| T4-θ SPD, % | -9,213 | 0,052 | -1,974 |
| T3-θ SPD, % | 5,164 | 0,050 | 1,428 |
| F3-θ SPD, % | -8,569 | 0,040 | -0,137 |
| P3-θ SPD, % | -0,950 | 0,036 | -0,152 |
| O1-θ SPD, % | -2,474 | 0,032 | -0,373 |
| θ rhythm Amplitude, μV | 10,914 | 0,028 | 1,951 |
| F4-α SPD, % | 6,236 | 0,026 | 0,387 |
| T6-δ SPD, $\mu V^2/Hz$ | -5,986 | -0,057 | -0,007 |
| P3-δ SPD, % | 5,175 | -0,056 | 0,214 |
| F4-δ SPD, $\mu V^2/Hz$ | 4,218 | -0,056 | 0,005 |
| O1-δ SPD, % | -8,847 | -0,051 | -0,382 |
| F3-δ SPD, $\mu V^2/Hz$ | 9,721 | -0,048 | 0,008 |
| T6-δ SPD, % | 4,344 | -0,042 | 0,161 |
| Eigenvalue | 19,84 | Constant | -60,62 |

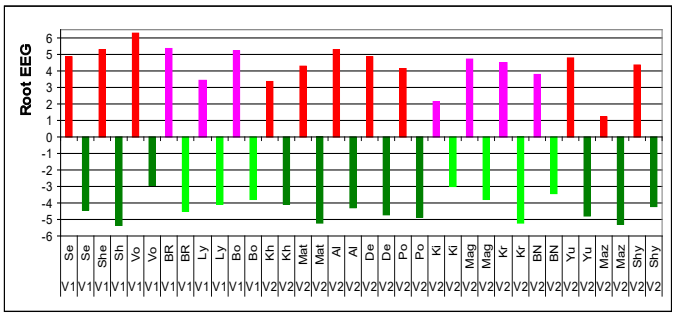


**Fig. 6. Individual values of the canonical discriminant EEGs root before and after four-day electrostimulation course with the devices "VEB-1" and "VEB-2" at females and males. Below the columns are the codes of the volunteers**

Therefore, the characteristic manifestations of the effect of electrical stimulation are: leveling of right-hand Lateralization and normalizing decrease in the increased of the Amplitude of the **θ-rhythm** and its SPD at the loci F3, F7, F8, T3, T4, T6, P3, O1 and O2; further increase of SPD of **δ-rhythm** in loci F3, F4, T6, P3 and O1 as well as further decrease of SPD **F4-α**; reversion of the increased level of **Entropy** in loci Fp1, F4, C3 and P3 to the lowered level.

Retrospective clustering of volunteers by gender and applied modification of the device indicates the absence of significant differences in the set of discriminant EEG parameters between women and men both before and after the course of electrical stimulation of both devices (Fig. 7).

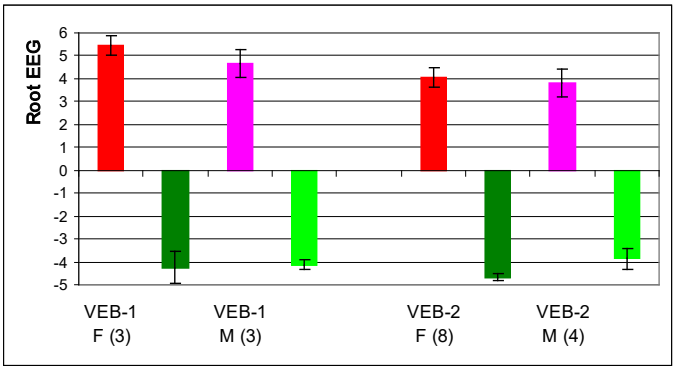


**Fig. 7. Average values (Mean±SE) of the canonical discriminant root EEG before and after four-day electrostimulation course with the devices "VEB-1" and "VEB-2" at women (F) and men (M)**

The application of the parameters of classification functions (Table 4) makes it possible to **unmistakably** recognize retrospectively when the EEG was registered: before or after the course of electrical stimulation.

**Table 4. Coefficients and Constants for Classification Functions**

| Variables currently in the model | Before | After |
|---|---|---|
| C3 SPD Entropy | 1333 | 1155 |
| F8-θ SPD, % | 0,408 | 0,234 |
| F3-θ SPD, % | -9,983 | -8,797 |
| P3 SPD Entropy | 3150 | 2738 |
| P3-θ SPD, % | -3,320 | -2,003 |
| θ rhythm Amplitude, μV | 145,6 | 128,8 |
| O1-θ SPD, % | -21,45 | -18,23 |
| F3-δ SPD, $\mu V^2/Hz$ | 0,539 | 0,472 |
| O1-δ SPD, % | -26,89 | -23,58 |
| T4-θ SPD, % | -134,9 | -117,9 |
| F8-θ SPD, $\mu V^2/Hz$ | 25,01 | 21,68 |
| θ rhythm Laterality Index, % | 7,393 | 6,431 |
| T3-θ SPD, % | 105,3 | 92,98 |
| P3-δ SPD, % | 16,42 | 14,56 |
| F4-α SPD, % | 27,94 | 24,60 |
| F4-δ SPD, $\mu V^2/Hz$ | 0,409 | 0,366 |
| T6-δ SPD, % | 10,954 | 9,557 |
| T6-δ SPD, $\mu V^2/Hz$ | -0,425 | -0,364 |
| Fp1 SPD Entropy | 1100 | 994,7 |
| T6-θ SPD, % | -41,57 | -35,93 |
| F7-θ SPD, % | -25,74 | -23,39 |
| F4 SPD Entropy | -929,2 | -750,1 |
| O2-θ SPD, % | 9,516 | 6,388 |
| Constants | -2531 | -2006 |

Secondly, we will consider significant or noteworthy changes in HRV parameters, as well as immune, biophysical and metabolic (Tables 5 and 6).

Regarding HRV the characteristic manifestations of the effect of electrical stimulation are: a decrease in elevated levels of **sympathetic** tone markers (LFnu and AMo) and an increase in decreased levels of **vagus** tone markers (RMSSD, HF, TNN and $pNN_{50}$), that is vagotonic shift of sympatho-vagus balance indicex (LF/HF, Bayevsiy's SI, Centralization Index), but without normalization. This is accompanied by a normalizing increase in the reduced entropy of the HRV spectrum.

Among the biophysical parameters revealed a insignificant increase in Electrokinetic Index and significant decrease in the increased electrical conductivity of the skin at the point of acupuncture MC (AVL) on the right, which led to the reversion of its Lateralization.

The Electrokinetic Index reflects the integral state of the organism [Shakhbazov VG, 2000], which is documented by its relationships with the parameters of EEG, HRV, Immunity, Metabolism, etc. [Kyrylenko IG, 2018,2018a]. The point of acupuncture MC (AVL) reflects the state of Immunity [Hubyts'kyi VY et al, 2013]. Therefore, favorable changes in the parameters of **Immunity**, especially an increase in the Killing Index of Neutrophils versus both Escherichia coli and Staphylococcus aureus, as well as level of CIC and T-killers, are quite expected for us.

**Table 5. Discriminant Function Analysis Summary for HRV, Immune, Biophysic&Metabolic Variables**
Step 9, N of vars in model: 9; Grouping: 2 grps
Wilks' Lambda: 0,467; approx. $F_{(9,3)}$=3,3; p=0,008

| Variables currently in the model | Reference value (36) | Average value | | Wilks' statistics parameters | | | | |
|---|---|---|---|---|---|---|---|---|
| | | Before (18) | After (18) | Wilks' Λ | Partial Λ | F-remove | p-level | Tolerancy |
| Killing Index vs Escherichia coli, % | 62,0 | 34,7 | 40,0 | 0,670 | 0,697 | 11,3 | 0,002 | 0,542 |
| Popovych's Leukocytary Strain Index | 0,07 | 0,15 | 0,25 | 0,532 | 0,878 | 3,60 | 0,069 | 0,622 |
| Klimov's Atherogenicity Coefficient | 2,97 | 2,45 | 2,65 | 0,486 | 0,961 | 1,04 | 0,316 | 0,736 |
| Spectral Power of LFnu, % | 65,4 | 84,0 | 76,8 | 0,575 | 0,813 | 6,00 | 0,021 | 0,310 |
| LF/HF ratio HRV | 2,87 | 7,09 | 4,49 | 0,517 | 0,905 | 2,74 | 0,110 | 0,288 |
| EC AP MC (AVL) Right, units | 58,0 | 63,3 | 61,2 | 0,518 | 0,902 | 2,82 | 0,105 | 0,591 |
| Amplitude of Mode HRV, % | 38,9 | 52,3 | 47,6 | 0,544 | 0,859 | 4,26 | 0,049 | 0,111 |
| Bayevskiy's Stress Index, ln units | 4,90 | 5,21 | 5,07 | 0,516 | 0,906 | 2,70 | 0,113 | 0,100 |
| EC AP MC(AVL) Laterality Index, % | 0 | 0,2 | -0,3 | 0,508 | 0,920 | 2,26 | 0,145 | 0,636 |
| **Variables currently not in the model** | | **Before** | **After** | **Wilks' Λ** | **Partial Λ** | **F to enter** | **p-level** | **Tolerancy** |
| RMSSD HRV, msec | 27,3 | 17,4 | 22,0 | 0,461 | 0,986 | 0,35 | 0,562 | 0,380 |
| Entropy of HRV | 0,798 | 0,710 | 0,775 | 0,463 | 0,991 | 0,24 | 0,632 | 0,643 |
| Spectral Power of HF band, % | 13,8 | 7,4 | 11,3 | 0,464 | 0,994 | 0,16 | 0,692 | 0,414 |
| Spectral Power of HF band, msec$^2$ | 346 | 134 | 209 | 0,464 | 0,994 | 0,15 | 0,700 | 0,452 |
| Triangulary Index HRV, units | 11,2 | 9,7 | 10,7 | 0,465 | 0,994 | 0,14 | 0,710 | 0,076 |
| pNN$_{50}$, % | 9,8 | 1,94 | 3,72 | 0,465 | 0,995 | 0,13 | 0,726 | 0,529 |
| Electrokinetic Index, % | 41,3 | 41,3 | 42,5 | 0,466 | 0,997 | 0,06 | 0,804 | 0,594 |
| $CD8^+CD3^+$ T-Lymphocytes, % | 23,5 | 20,5 | 21,9 | 0,466 | 0,997 | 0,06 | 0,802 | 0,564 |
| Circulating Immune Complicex, units | 45 | 33 | 41 | 0,467 | 0,999 | 0,02 | 0,888 | 0,750 |
| Killing Index vs Staphyloc. aureus, % | 58,9 | 41,1 | 49,3 | 0,467 | 1,000 | 0,00 | 0,963 | 0,587 |
| (VLF+LF)/HF as Centralization Index | 7,0 | 16,8 | 10,3 | 0,456 | 0,977 | 0,60 | 0,446 | 0,302 |
| High Density LP Cholesterol, mM/L | 1,40 | 1,75 | 1,61 | 0,465 | 0,996 | 0,11 | 0,741 | 0,396 |
| C-Reactive Protein, mg/L | 2,18 | 2,90 | 2,79 | 0,466 | 0,998 | 0,06 | 0,809 | 0,711 |

**Table 6. Summary of Stepwise Analysis for HRV, Immune, Biophysic&Metabolic Variables (ranked by criterion Lambda)**

| Variables currently in the model | F to enter | p-level | Lambda | F-value | p-level |
|---|---|---|---|---|---|
| Killing Index vs Escherichia coli, % | 7,55 | 0,010 | 0,818 | 7,55 | 0,009 |
| Spectral Power of LFnu, % | 5,82 | 0,022 | 0,696 | 7,22 | 0,003 |
| Popovych's Leukocytary Strain Index | 2,36 | 0,135 | 0,648 | 5,79 | 0,003 |
| Amplitude of Mode HRV, % | 1,25 | 0,272 | 0,623 | 4,69 | 0,004 |
| Bayevskiy's Stress Index, ln units | 2,61 | 0,117 | 0,573 | 4,47 | 0,004 |
| LF/HF ratio HRV | 1,86 | 0,184 | 0,539 | 4,14 | 0,004 |
| EC AP MC(AVL) Right, units | 1,15 | 0,293 | 0,517 | 3,73 | 0,006 |
| EC AP MC(AVL) Laterality Index, % | 1,74 | 0,198 | 0,486 | 3,57 | 0,006 |
| Klimov's Atherogenicity Coefficient | 1,04 | 0,316 | 0,467 | 3,29 | 0,008 |
| r*=0,730; Wilks' Λ=0,467; $\chi^2_{(9)}$=22,4; p=0,008 | | | | | |
| Squared Mahalanobis Distance=4,56; F=3,29; p=0,008 | | | | | |

Under the identified circumstances, we consider further increase of the Popovych's Leukocytary Strain Index to be favorable. And the increase within the norm of reduced Klimov's Atherogenicity Coefficient due to the decrease within the norm of the increased level of High Density LP Cholesterol we interpret as at least neutral.
Unfortunately, due to lack of funding, we could not determine the level of pro-inflammatory cytokines. Therefore, it is hoped that the tendency to decrease the level of C-Reactive Protein is a predictor of the anti-inflammatory effect of electrical stimulation.
Leaving without comments Tables 7 and 8, we emphasize that the parameters included in the discriminant model when using classification functions allow to retrospectively recognize the initial state of the organism with an accuracy of 88,9% (2 errors), and the final even less (83,3%, 3 errors) against the background of error-free recognition by EEG parameters.

**Table 7. Standardized, Structural and Raw Coefficients and Constant for for HRV, Immune, Biophysic&Metabolic Variables (ranked by Structural coefficient)**

| | Coefficients | | |
|---|---|---|---|
| Variables currently in the model | Standardized | Structural | Raw |
| Killing Index vs Escherichia coli, % | 1,024 | 0,441 | 0,175 |
| Popovych's Leukocytary Strain Index | 0,606 | 0,228 | 2,724 |
| Klimov's Atherogenicity Coefficient | 0,314 | 0,228 | 0,712 |
| Spectral Power of LFnu, % | -1,066 | -0,369 | -0,114 |
| LF/HF ratio HRV | 0,788 | -0,286 | 0,179 |
| EC AP MC(AVL) Right, units | -0,558 | -0,177 | -0,095 |
| Amplitude of Mode HRV, % | -1,544 | -0,157 | -0,106 |
| Bayevskiy's Stress Index, ln units | 1,331 | -0,106 | 2,093 |
| EC AP MC(AVL) Laterality Index, % | 0,486 | -0,062 | 13,840 |
| Eigenvalue | 1,14 | Constant | -0,348 |

**Table 8. Coefficients and Constants for Classification Functions for HRV, Immune, Biophysic&Metabolic Variables**

| Variables currently in the model | Before | After |
|---|---|---|
| Killing Index vs Escherichia coli, % | -0,753 | -0,391 |
| Spectral Power of LFnu, % | 2,333 | 2,098 |
| Popovych's Leukocytary Strain Index | 44,35 | 50,01 |
| Amplitude of Mode HRV, % | -2,041 | -2,261 |
| Bayevskiy's Stress Index, ln units | 65,38 | 69,73 |
| LF/HF ratio HRV | -4,592 | -4,219 |
| EC AP MC(AVL) Right, units | 1,531 | 1,334 |
| EC AP MC(AVL) Laterality Index, % | -92,00 | -63,28 |
| Klimov's Atherogenicity Coefficient | 24,44 | 25,92 |
| Constants | -267,7 | -268,4 |

If the GDV parameters are offered for the program from the information field, the discriminant model will absorb 10 of them, which will displace a number parameters of HRV, Immunity and Metabolism from the previous model (Tables 9-12), but will provide an **error-free** retrospective classification (Table 13).

**Table 9. Discriminant Function Analysis Summary for GDV, HRV, Immune, Biophysic and Metabolic Variables**

Step 16, N of vars in model: 9; Grouping: Before&After electrostimulation

Wilks' Lambda: 0,114; approx. $F_{(16,2)}$=9,2; $p<10^{-5}$

| | Refer value (36) | Average value | | Wilks' statistics parameters | | | | |
|---|---|---|---|---|---|---|---|---|
| Variables currently in the model | | Before (18) | After (18) | Wilks' Λ | Partial Λ | F-remove | p-level | Tole-rancy |
| Killing Index vs Escher. coli, % | 62,0 | 34,7 | 40,0 | 0,142 | 0,806 | 4,57 | 0,046 | 0,375 |
| Spectral Power of LFnu, % | 65,4 | 84,0 | 76,8 | 0,167 | 0,684 | 8,78 | 0,008 | 0,244 |
| Chakra 3 Asymmetry (f) | 0,01 | -0,05 | 0,04 | 0,180 | 0,636 | 10,86 | 0,004 | 0,262 |
| RMSSD HRV, msec | 27,3 | 17,4 | 22,0 | 0,208 | 0,551 | 15,50 | $<10^{-3}$ | 0,293 |
| Chakra 2 Asymmetry (f) | 0,02 | -0,04 | -0,14 | 0,226 | 0,505 | 18,59 | $<10^{-3}$ | 0,307 |
| Chakra 2 Energy | -0,07 | 0,13 | -0,01 | 0,126 | 0,908 | 1,94 | 0,180 | 0,038 |
| Chakra 7 Energy (f) | 0,02 | 0,07 | 0,11 | 0,227 | 0,503 | 18,78 | $<10^{-3}$ | 0,054 |
| Area GDI Frontal, kpixels | 24,9 | 26,2 | 25,0 | 0,187 | 0,610 | 12,15 | 0,003 | 0,067 |
| Entropy GDI Left | 3,93 | 3,82 | 3,74 | 0,216 | 0,529 | 16,91 | $<10^{-3}$ | 0,252 |
| Symmetry GDI (f), % | 94,7 | 93,4 | 92,6 | 0,121 | 0,945 | 1,12 | 0,304 | 0,237 |
| Chakra 7 Energy | -0,11 | 0,08 | -0,03 | 0,150 | 0,763 | 5,91 | 0,025 | 0,036 |
| Chakra 4 Asymmetry | 0,03 | -0,05 | 0,10 | 0,144 | 0,793 | 4,95 | 0,039 | 0,393 |
| Chakra 1 Asymmetry (f) | -0,01 | -0,17 | -0,07 | 0,140 | 0,819 | 4,21 | 0,054 | 0,275 |
| EC AP MC(AVL) Lateral. Ind, % | 0,0 | 0,2 | -0,3 | 0,121 | 0,948 | 1,05 | 0,318 | 0,613 |
| LF/HF ratio HRV | 2,87 | 7,09 | 4,49 | 0,127 | 0,897 | 2,18 | 0,156 | 0,243 |
| GDI Shape Coefficient Left (f) | 11,5 | 13,0 | 13,6 | 0,124 | 0,925 | 1,55 | 0,228 | 0,099 |
| **Variables currently not in the model** | | **Before** | **After** | **Wilks' Λ** | **Partial Λ** | **F to enter** | **p-level** | **Tole-rancy** |
| Klimov's Atherogenicity Coefficient | 2,97 | 2,45 | 2,65 | 0,113 | 0,992 | 0,15 | 0,703 | 0,517 |
| Bayevskiy's Stress Index, ln units | 4,90 | 5,21 | 5,07 | 0,114 | 0,999 | 0,02 | 0,893 | 0,334 |
| Spectral Power of HF band, msec$^2$ | 346 | 134 | 209 | 0,114 | 0,999 | 0,03 | 0,875 | 0,168 |
| EC AP MC(AVL) Right, units | 58,0 | 63,3 | 61,2 | 0,111 | 0,969 | 0,58 | 0,455 | 0,461 |
| Popovych's Leukocyt Strain Index | 0,07 | 0,15 | 0,25 | 0,114 | 0,999 | 0,01 | 0,918 | 0,583 |
| Entropy of GDI Right | 3,85 | 3,80 | 3,76 | 0,110 | 0,961 | 0,74 | 0,402 | 0,550 |
| Chakra 3 Energy | -0,09 | 0,03 | -0,07 | 0,112 | 0,977 | 0,43 | 0,522 | 0,154 |
| Amplitude of Mode HRV, % | 38,9 | 52,3 | 47,6 | 0,111 | 0,998 | 0,57 | 0,450 | 0,460 |

**Table 10. Summary of Stepwise Analysis for GDV, HRV, Immune, Biophysic and Metabolic Variables (ranked by criterion Lambda)**

| Variables currently in the model | F to enter | p-level | Lambda | F-value | p-level |
|---|---|---|---|---|---|
| Killing Index vs Escherichia coli, % | 7,55 | 0,010 | 0,818 | 7,55 | 0,010 |
| Spectral Power of LFnu, % | 5,82 | 0,022 | 0,696 | 7,22 | 0,003 |
| Chakra 3 Asymmetry (f) | 5,98 | 0,020 | 0,586 | 7,53 | $<10^{-3}$ |
| RMSSD HRV, msec | 3,56 | 0,069 | 0,526 | 6,99 | $<10^{-3}$ |
| Chakra 2 Asymmetry (f) | 2,93 | 0,098 | 0,479 | 6,52 | $<10^{-3}$ |
| Chakra 2 Energy | 3,34 | 0,078 | 0,430 | 6,42 | $<10^{-3}$ |
| Chakra 7 Energy (f) | 5,63 | 0,025 | 0,358 | 7,18 | $<10^{-4}$ |
| Area GDI Frontal, kpixels | 7,48 | 0,011 | 0,280 | 8,67 | $<10^{-5}$ |
| Entropy GDI Left | 2,99 | 0,096 | 0,251 | 8,61 | $<10^{-5}$ |
| Symmetry GDI (f), % | 5,40 | 0,029 | 0,207 | 9,60 | $<10^{-5}$ |
| Chakra 7 Energy | 2,78 | 0,108 | 0,185 | 9,61 | $<10^{-5}$ |
| Chakra 4 Asymmetry | 4,01 | 0,057 | 0,158 | 10,2 | $<10^{-6}$ |
| Chakra 1 Asymmetry (f) | 2,12 | 0,159 | 0,144 | 10,1 | $<10^{-5}$ |
| EC AP MC(AVL) Laterality Index, % | 1,72 | 0,204 | 0,133 | 9,79 | $<10^{-5}$ |
| LF/HF ratio HRV | 1,48 | 0,237 | 0,124 | 9,44 | $<10^{-5}$ |
| GDI Shape Coefficient Left (f) | 1,55 | 0,228 | 0,114 | 9,20 | $<10^{-5}$ |
| r*=0,941; Wilks' Λ=0,114; $\chi^2_{(16)}$=56,4; $p<10^{-5}$ | | | | | |
| Squared Mahalanobis Distance=31,0; F=9,2; $p<10^{-5}$ | | | | | |

**Table 11. Standardized, Structural and Raw Coefficients and Constant for GDV, HRV, Immune, Biophysic and Metabolic Variables (ranked by Structural coefficient)**

| | Coefficients | | |
|---|---|---|---|
| Variables currently in the model | Standardized | Structural | Raw |
| Killing Index vs Escherichia coli, % | 0,764 | 0,169 | 0,130 |
| RMSSD HRV, msec | 1,316 | 0,103 | 0,161 |
| Chakra 3 Asymmetry (f) | 1,252 | 0,097 | 7,907 |
| Chakra 1 Asymmetry (f) | -0,863 | 0,080 | -3,588 |
| Chakra 4 Asymmetry | 0,770 | 0,072 | 1,996 |
| GDI Shape Coefficient Left (f) | 0,926 | 0,074 | 0,688 |
| Chakra 7 Energy (f) | 3,233 | 0,030 | 12,67 |
| Spectral Power of LFnu, % | -1,211 | -0,141 | -0,129 |
| LF/HF ratio HRV | 0,692 | -0,110 | 0,157 |
| Entropy GDI Left | -1,452 | -0,086 | -9,356 |
| Symmetry GDI (f), % | -0,514 | -0,083 | -0,278 |
| Chakra 2 Asymmetry (f) | -1,349 | -0,070 | -5,311 |
| Chakra 2 Energy | -1,664 | -0,059 | -3,882 |
| Chakra 7 Energy | -2,728 | -0,050 | -7,100 |
| Area GDI Frontal, kpixels | 2,564 | -0,048 | 0,56 |
| EC AP MC(AVL) Laterality Index, % | 0,311 | -0,024 | 8,847 |
| Eigenvalue | 7,744 | Constant | 37,47 |

**Table 12. Coefficients and Constants for Classification Functions for GDV, HRV, Immune, Biophysic and Metabolic Variables**

| Variables currently in the model | Before | After |
|---|---|---|
| Killing Index vs Escherichia coli, % | -2,415 | -1,709 |
| Spectral Power of LFnu, % | 5,603 | 4,904 |
| Chakra 3 Asymmetry (f) | -139,1 | -96,35 |
| RMSSD HRV, msec | -6,233 | -5,360 |
| Chakra 2 Asymmetry (f) | -112,3 | -141,0 |
| Chakra 2 Energy | -282,4 | -303,4 |
| Chakra 7 Energy (f) | 407,6 | 476,2 |
| Area GDI Frontal, kpixels | 12,01 | 15,02 |
| Entropy GDI Left | 835,6 | 785,0 |
| Symmetry GDI (f), % | 154,5 | 153,0 |
| Chakra 7 Energy | 590,2 | 551,8 |
| Chakra 4 Asymmetry | -54,27 | -43,481 |
| Chakra 1 Asymmetry (f) | -187,8 | -207,2 |
| EC AP MC(AVL) Laterality Index, % | -1406 | -1358 |
| LF/HF ratio HRV | 8,316 | 9,167 |
| GDI Shape Coefficient Left (f) | 214,2 | 217,8 |
| Constants | -10577 | -10375 |

**Table 13. Classification Matrix**
Rows: Observed classifications
Columns: Predicted classifications

| | Percent correct | Before | After |
|---|---|---|---|
| Before | 100 | **18** | 0 |
| After | 100 | 0 | **18** |
| Total | 100 | **18** | **18** |

If the biophysical (Area and Shape of GDI and its Symmetry) and informational (GDI Entropy) GDV parameters are more or less tolerantly perceived by scientists who follow the paradigm of Western medicine, then for the **Chakras**, which are almost the main attribute of Eastern medicine, we risk further obstruction.

According to existent paradigm, **Chakras** are power centers, related to the endocrine glands and neural plexus as well as to some organs. In particular, the **first Chakra** is related to the testicles and sacral plexus, **second Chakra** to the ovaries, adrenals and kidneys, **third Chakra** to spleen, liver and solar plexus, **fourth Chakra** to thymus, heart and cardial plexus, **fifth Chakra** to thyroid and parathyroid glands, **sixth Chakra** to pituitary gland and brain, **seven Chakra** to pineal gland [Puchko LG, 2004].

The method we use evaluates the Energy and Asymmetry of the **virtual** Chakras, calculated by the program based on the GDV parameters of the skin of ten fingers.

The effects of electrical stimulation can be divided into the following networks. First, it is almost complete normalization of the initially increased GDI Area in the Frontal projection and Chakra 3 (**Spleen!**) Energy. Second, it is a normalizing decrease in the initially increased Energy of Chakra 2 (**Steroides!**) and Chakra 7(f). Third, it is a normalizing right-hand shift of more or less pronounced left-sided Asymmetry of Chakra 1(f) and Chakra 3(f). These effects should be clearly interpreted as physiologically beneficial.

The second set is created by quasi-normal (Chakra 4 (**Thymus!**) Asymmetry, Chakra 7 Energy(f) and elevated (Shape Coefficient Left,f) parameters, which increase after electrical stimulation, the physiological assessment of changes of which we will leave without comment.

The third set is formed by initially reduced levels of GDI Entropy in the Right and Left projections, which continue to decrease after electrical stimulation, as well as quasi-symmetric Chakra 2(f), which is transformed into left-asymmetric. If the decrease in Entropy can still be assessed positively, then the price change of the latter parameters will wait.

Fig. 8 demonstrates that more or less pronounced changes in these parameters occur in all volunteers without exception.

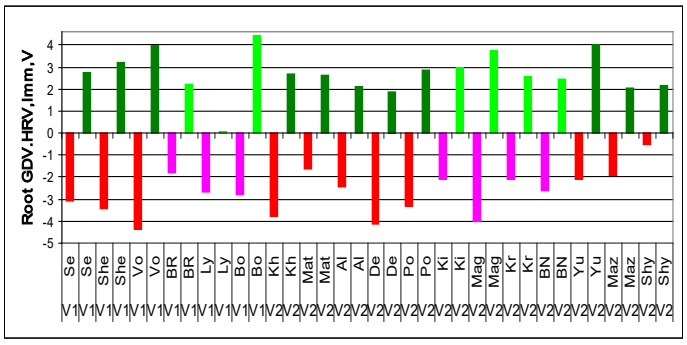


**Fig. 8. Individual values of the canonical discriminant root of GDV, HRV&Immune parameters before and after four-day electrostimulation course with the devices "VEB-1" and "VEB-2" at females and males**

The effects on the set of GDV, HRV and Immune parameters are almost equally pronounced in people of both sexes when using both devices (Fig. 9).

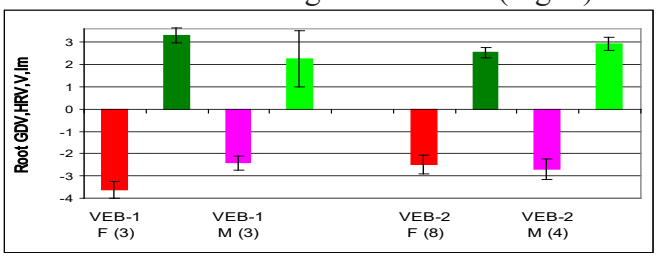


**Fig. 9. Average values (Mean±SE) of the canonical discriminant root of GDV, HRV&Immune parameters before and after four-day electrostimulation course with the devices "VEB-1" and "VEB-2" at women (F) and men (M)**

We consider it necessary to return to the Tracey's KJ [2007] scheme of immunological homunculus by which the neural structures that are projected onto definite loci responsible for certain immune functions, that is the immune compartment **cytokines** release (F3 and/or F4), activation of memory B cells (Fp1 and/or Fp2), dendritic cells maturation (T3 and/or T4), regulation of T cells (T5 and/or T6), clonal expansion (P3 and/or P4) and late **cytokine** release (P? or O?).

It is believed that a hippocampus is projected at the C3 and C4 loci, and the T3 and T4 loci reflect the activity of the amygdala [Romodanov AP, 1993]. The prefrontal loci record the activity of anterior cingulate [Cahn BR, Polish J., 2006] as well as orbito-frontal cortex. It is shown that the cortical thickness of an area within these regions positively correlated with two HRV-markers of parasympathetic activity both HF [Winkelmann T et al, 20107] and RMSSD [Yoo HJ et al, 2016]. It is shown significantly positive correlations between HFnu and Fz-θ, FCz-θ and Cz-θ [Tang et al, 2009]. Previously we [Popovych IL et al, 2013,2014] also found correlations between HFnu and F4-θ and P4-θ, between HF relative and Fp1-θ and P4-θ also between RMSSD and P4-θ. Prinsloo GE et al [2013] found that less pronounced changes in HRV, due to work-related stress, accompanied by higher relative SPD Fz-θ, Pz-θ and Cz-θ, lower fronto-central relative β power and higher θ/β ratio. It is also perfectly consistent with our [Popovych IL et al, 2013,2014] data on a negative correlation LFnu, LFr and LF/HF with F4-θ, P4-θ, F7-θ, F8-θ and positive - with F7-β and F8-β - on the one hand, and a positive correlation HFr with Fp1-θ and P4-θ and negative - with P4-β - on the other side.

We hope that our results complement and specify the concept according to which the hippocampus and amygdale are limbic brain structures that process experiences by interfacing with lower vegetative brain areas, such as the hypothalamus and brainstem, and higher cortical areas, particularly within the prefrontal cortex. Cortical structures providing inhibitory control over limbic and brainstem sympathoexcitatory circuits, indeed, disruption of prefrontal activity leads to disinhibition of sympathoexcitatory circuits, with a resultant decrease in vagally-mediated HRV [Carnevali L et al, 2018]. In particular, we found that electrostimulation-induced vagotonic shift of sympatho-vagus balance is associated with activation of neurons that generate δ-rhythm, whereas the activity of generating θ-rhythm neurons that are projected at the same EEG loci, is reduced.

**ACKNOWLEDGMENT**

We express sincere gratitude to administration JSC "Truskavets'kurort" for help in recording EEG and HRV and carrying out immune analyzes. Special thanks to the volunteers.

**ACCORDANCE TO ETHICS STANDARDS**

Tests in volunteers are conducted in accordance with positions of Helsinki Declaration 1975, revised and complemented in 2002, and directive of National Committee on ethics of scientific researches. During realization of tests from all participants the informed consent is got and used all measures for providing of anonymity of participants.

**REFERENCES**

1. Babelyuk NV, Babelyuk VYe, Dubkowa GI, Kikhtan VV, Musiyenko VY, Hubyts'kyi VY, Dobrovolsky YG, Korsunskyi IH, Kovbasnyuk MM, Korolyshyn TA, Popovych IL. Influence of the course of electrostimulation by the device "ES-01.9 WEB" on some functional systems of the organism of practically healthy men [in Ukrainian]. In: Proceedings VIII Scientific Conference "Issues of pathology in conditions of extreme factors action on the body" (Ternopil', 1-2 October 2015). Ternopil'. 2015: 5-6.
2. Babelyuk NV, Babelyuk VYe, Dubkowa GI, Korolyshyn TA, Kikhtan VV, Dobrovolsky YG, Korsuns'kyi IH, Kovbasnyuk MM. Electrical stimulation with the device "ES-01.9 WEB" activates some functional systems of the body of practically healthy men [in Ukrainian]. In: Valeology: current status, trends and persrectives

of development. Abstracts. XIV Intern. scient. and practical. conf. (Kharkiv-Drohobych, 14-16 April 2016). Kharkiv: VN Karazin KhNU. 2016: 198-200.
3. Babelyuk NV, Babelyuk VYe, Dubkowa GI, Kikhtan VV, Musiyenko VY, Hubyts'kyi VY, Dobrovolsky YG, Korsuns'kyi IH, Kovbasnyuk MM, Korolyshyn TA, Popovych IL. Modulation of functional systems of practically healthy men by the course of electrostimulation [in Ukrainian]. In: IX International symposium "Actual problems of biophysical medicine" (Kyiv, 12-15 May 2016). Kyiv: OO Bohomolets' Institute of Physiology; 2016: 10-11.
4. Babelyuk NV, Babelyuk VY, Kikhtan VV, Popovych IL, Burkovs'ka MM, Dobrovolsky YG, Korsuns'kyi IH, Kindzer BM, Zukow W. The influence of the course of electrostimulation by the device "VEB-1" on metabolic parameters at practically healthy males. Experimental and Clinical Physiology and Biochemistry. 2018; 4(84): 11-17.
5. Babelyuk VYe. The parameters of gas discharge visualization (kirlianogram) appropriately associated with some psychophysiological and endocrine parameters of healthy men. Medical Hydrology and Rehabilitation. 2013; 11(1): 21-30.
6. Babeluk VE. The patent of Ukraine for utility model 105875 Portable device for electrotherapy and stimulation, 2016.
7. Babelyuk VYe, Dubkova GI, Korolyshyn TA, Zukow W, Popovych IL. The correlationships between parameters of gas discharge visualization and principal neuroendocrine factors of adaptation. In: Pathophysiology and Pharmacy: ways of integration. Abstracts VII National Congress of Pathophysiologists Ukraine with international participation (5-7 October 2016). Kharkiv. NPhU; 2016: 8-8.
8. Babelyuk VY, Dobrovolsky YuG, Popovych IL, Korsunskiy IG. Generator for electrotherapy and stimulation oh human nerve centers [in Russian]. Tekhnologiya i Konstruirovaniye v Elektronnoy Apparature. 2017; 1-2: 23-27.
9. Babelyuk VYe, Dubkowa GI, Korolyshyn TA, Holubinka SM, Dobrovolsky YG, Zukow W, Popovych IL. Operator of Kyokushin Karate via Kates increases synaptic efficacy in the rat Hippocampus, decreases C3-θ-rhythm SPD and HRV Vagal markers, increases virtual Chakras Energy in the healthy humans as well as luminosity of distilled water in vitro. Preliminary communication. Journal of Physical Education and Sport. 2017; 17(1): 383-393.
10. Babelyuk VE, Gozhenko AI, Dubkova GI, Babelyuk NV, Zukow W, Kovbasnyuk MM, Popovych IL. Causal relationships between the parameters of gas discharge visualization and principal neuroendocrine factors of adaptation. Journal of Physical Education and Sport. 2017; 17(2): 624-637.
11. Babelyuk VYe, Babelyuk NV, Popovych IL, Dobrovolsky YuG, Korsuns'kyi IH, Korolyshyn TA, Kindzer BM, Zukow W. Influence of the course of electrostimulation by the device "VEB-1" on parameters of electroencephalogram at practically healthy males. Journal of Education, Health and Sport. 2018; 8(4): 195-206.
12. Babelyuk VY, Dubkova HI, Korolyshyn TA, Mysula IR, Popovych DV, Popovych IL, Zukow W. Relationships between caused by Kozyavkin© method changes in parameters of manual function and electroencephalogram, heart rate variability as well as gas discharge visualization in children with spastic form of cerebral palsy. Journal of Education, Health and Sport. 2018; 8(4): 159-194.
13. Babelyuk VYe, Popadynets' OO, Dubkova GI, Zukow W, Muszkieta R, Gozhenko OA, Popovych IL. Entropy of gas-discharge image correlates with the entropies of EEG, immunocytogram and leukocytogram but not HRV. Pedagogy and Psychology of Sport. 2020; 6(2): 30-39.
14. Baevskiy RM, Ivanov GG. Heart Rate Variability: theoretical aspects and possibilities of clinical application [in Russian]. Ultrazvukovaya i funktsionalnaya diagnostika. 2001; 3: 106-127.
15. Baptista AF, Maciel ABR, Okano AH, Moreira A, Campos ACP, Fernandes AM, Brunoni AR, Tanaka C, Andrade DC, Machado DGS, Morya E, Trujillo E, Monte-Silva K, Sa KN, Baptista INSF, Goulardins JB, Sudbrack-Oliveira P, Carvalho P, Moreira RJD, Pagano RM, Shinjo SK, Zana Y. Neuromodulation and inflammatory reflex: Perspectives on the use of non-invasive neuromodulation in the management of disorders related to COVID-19. Preprint. 2020. May: 31p.
16. Barylyak LG., Malyuchkova RV, Tolstanov OB,

Tymochko OB, Hryvnak RF, Uhryn MR. Comparative estimation of informativeness of leukocytary index of adaptation by Garkavi and by Popovych. Medical Hydrology and Rehabilitation. 2013; 11(1): 5-20.
17. Berntson GG, Bigger JT jr, Eckberg DL, Grossman P, Kaufman PG, Malik M, Nagaraja HN, Porges SW, Saul JP, Stone PH, Van der Molen MW. Heart Rate Variability: Origines, methods, and interpretive caveats. Psychophysiology. 1997; 34: 623-648.
18. Bikson M, Hanlon CA, Woods AJ, Gillic BT, Charvet L, Lamm C et al. Guidelines for TMS/tES clinical services and research through the COVID-19 pandemic. Brain Stimulation. 2020; 13: 1124-1149.
19. Borovikova LV, Ivanova S, Zhang M, Yang H, Botchkina GI, Watkins LR, Wang H, Abumrad N, Eaton JW, Tracey KJ. Vagus nerve stimulation attenuates the systemic inflammatory response to endotoxin. Nature. 2000; 405: 458-462.
20. Cahn BR, Polish J. Psychological bulletin meditation states and traits: EEG, ERP and neuroimaging studies. Psychol. Bull. 2006; 132: 180-211.
21. Carnevali L, Koenig J, Sgoifo A, Ottaviani C. Autonomic and brain morphological predictors of stress recilience. Front Neurosci. 2018; 12: 228.
22. Chavan SS, Pavlov VA, Tracey KJ. Mechanism and therapeutic relevance of neuro-immune communication. Immunity. 2017; 46: 927-942.
23. Chavan SS, Tracey KJ. Essencial Neuroscience in Immunology. J Immunol. 2017; 198: 3389-3397.
24. Douglas SD, Quie PG. Investigation of Phagocytes in Disease. Churchil. 1981. 110 p.
25. Fudium M, Qadri YJ, Ghadimi K, MacLeod DB, Malinger J, Piccini JP et al. Implication for neuromodulation therapy to control inflammation and related organ dysfunction in COVID-19. J Cardiovasc Transl Res. 2020. May 26: 1-6.
26. Gozhenko AI, Sydoruk NO, Babelyuk VYe, Dubkowa GI, Flyunt VR, Hubyts'kyi VYo, Zukow W, Barylyak LG, Popovych IL. Modulating effects of bioactive water Naftussya from layers Truskavets' and Pomyarky on some metabolic and biophysic parameters at humans with dysfunction of neuro-endocrine-immune complex. Journal of Education, Health and Sport. 2016; 6(12): 826-842.
27. Heart Rate Variability. Standards of Measurement, Physiological Interpretation, and Clinical Use. Task Force of ESC and NASPE. Circulation. 1996; 93(5): 1043-1065.
28. Hubyts'kyi VY, Humenna OP, Barylyak LG, Bolyukh VV, Popovych IL, Maluchkova RV. Eleeectro-skin resistance of points of acupuncture correlates with some parameters of neuroendocrine-immune complex [in Ukrainian]. Medical Hydrology and Rehabilitation. 2013; 11(2): 4-11.
29. Hyoju SK, Alverdy JC, Zagorina O, Goor van H. SARS-CoV-2 and the sympathetic immune response: dampening inflammation with antihypertensive drugs (Clonidine and Labetalol). Research Proposal. 2020. April. DOI: 10.13140/RG.2.2.36574.79681.
30. Kindzer BM, Babelyuk VY, Babelyuk NV, Popovych IL, Dubkova GI, Dobrovolsky YG, Korsuns'kyi IH, Korolyshyn TA, Litosh S, Kindzer H, Zukow W. The device for electrostimulation "VEB-1" modulates parameters of electroencephalogram and gas discharge visualization. Science and society. Proc. of the 11th internat. confer. Acent Grafics Communications and Publishing. Hamilton, Canada. 2019: 159-171.
31. Klecka WR. Discriminant Analysis [trans. from English in Russian] (Seventh Printing, 1986). In: Factor, Discriminant and Cluster Analysis. Moskwa: Finansy i Statistika. 1989: 78-138.
32. Korneva EA (editor). Immunophysiology [in Russian]. St-Pb: Nauka. 1993. 684 p.
33. Korotkov KG. Basics GDV Bioelectrography [in Russian]. SPb. SPbGITMO(TU); 2001: 360 p.
34. Korotkov KG. Principles of Analysis in GDV Bioelectrography [in Russian]. SPb/ Renome; 2007: 286 p.
35. Korotkov KG. Energy Fields Electrophotonic Analysis in Humans and Nature. Second updated edition. Translated from Russian by the author. Edoted by Berney Williams and Lutz Rabe. 2014: 233 p.
36. Kozyavkina OV, Kozyavkina NV, Voloshyn TB, Hordiyevych MS, Lysovych VI, Babelyuk VY, Dubkova HI, Korolyshyn TA, Mysula IR, Popovych DV, Zukow W, Popovych IL. Caused by Kozyavkin© method changes in hand function parameters in children with spastic form of cerebral palsy and their EEGs, HRVs and GDVs accompaniments. Journal of Education, Health

and Sport. 2018; 8(10): 11-30.
37. Kozyavkina OV, Kozyavkina NV, Hordiyevych MS, Voloshyn TB, Lysovych VI, Babelyuk VY, Dubkova HI, Korolyshyn TA, Popovych DV, Mysula IR, Zukow W, Popovych IL. Forecasting caused by Kozyavkin© method changes in hand function parameters in children with spastic form of cerebral palsy at their baseline levels as well as EEGs, HRVs and GDVs. Achivements of Clinical and Experimental Medicine. 2018; 4: 17-35.
38. Kul'chyns'kyi AB**,** Kyjenko VM, Zukow W, Popovych IL. Causal neuro-immune relationships at patients with chronic pyelonephritis and cholecystitis**.** Correlations between parameters EEG, HRV and white blood cell count. Open Medicine. 2017; 12(1): 201-213.
39. Kul'chyns'kyi AB, Zukow W, Korolyshyn TA, Popovych IL. Interrelations between changes in parameters of HRV, EEG and humoral immunity at patients with chronic pyelonephritis and cholecystitis. Journal of Education, Health and Sport. 2017; 7(9): 439-459.
40. Kyrylenko IG. Changes in electrokinetic index of buccal epithelium correlated with changes in some parameters of EEG, HRV, hemodynamics and metabolism. Experimental and Clinical Physiology and Biochemistry. 2018; 2(82): 5-14.
41. Kyrylenko IG, Flyunt I-SS, Fil' VM, Zukow W, Popovych IL. Changes in electrokinetic index of buccal epithelium correlated with changes in some parameters of immunity and fecal microbiocenosis. Journal of Education, Health and Sport. 2018; 8(10): 168-170.
42. Lapovets' LYe, Lutsyk BD. Handbook of Laboratory Immunology [in Ukrainian]. L'viv. 2002. 173 p.
43. Nance DM, Sanders VM. Autonomic innervation and regulation of immune system (1987-2007). Brain Behav Immun. 2007; 21(6): 736-745.
44. Newberg AB, Alavi A, Baime M, Pourdehnad M, Santanna J, d'Aquili E. The measurement of regional cerebral blood flow during the complex cognitive task of meditation: a preliminary SPECT study. Psychiatry Research: Neuroimaging Section. 2001; 106: 113-122.
45. Ohtake Y, Hamada T, Murata T. et al. The assotiation between autonomic response status and the changes in EEG activity during mental arithmetic task. Rinsho Byori. 2007; 55(12): 1075-1079.
46. Pavlov VA, Chavan SS, Tracey KJ. Molecular and functional neuroscience in immunity. Annu Rev Immunol. 2018; 36: 783-812.
47. Popadynets' OO, Gozhenko AI, Zukow W, Popovych IL. Relationships between the entropies of EEG, HRV, immunocytogram and leukocytogram. Journal of Education, Health and Sport. 2019; 9(5): 651-666.
48. Popadynets' OO, Gozhenko AI, Badiuk NS, Zukow W, Kovbasnyuk MM, Korolyshyn TA, Popovych IL. Relationships between changes in entropy of the EEG and parameters of the immunity. Pedagogy and Psychology of Sport. 2020; 6(1): 24-40.
49. Popovych IL. Functional relationships between parameters of neuro-endocrine-immune complex at male rats [in Ukrainian]. Achivements of Clinical and Experimental Medicine. 2008; 2(9): 80-87.
50. Popovych IL. Feature of immunity by various constellations of hormones and autonomous regulation. In: Materials of the XXth Congress of the Ukrainian Physiological Society named after PG Kostyuk. Fiziol Zhurn. 2019; 65(3). Suppl: 184-184.
51. Popovych IL, Babelyuk VYe, Dubkova GI. Relations between the parameters bioelectrography (kirlianography) and heart rate variability and blood pressure [in Ukrainian]. Medical Hydrology and Rehabilitation. 2010; 8(1): 4-16.
52. Popovych IL, Lukovych YuS, Korolyshyn TA, Barylyak LG, Kovalska LB, Zukow W. Relationship between the parameters heart rate variability and background EEG activity in healthy men. Journal of Health Sciences. 2013; 3(4): 217-240.
53. Popovych IL, Kozyavkina OV, Kozyavkina NV, Korolyshyn TA, Lukovych YuS, Barylyak LG. Correlation between Indices of the Heart Rate Variability and Parameters of Ongoing EEG in Patients Suffering from Chronic Renal Pathology. Neurophysiology. 2014; 46(2): 139-148.
54. Popovych IL, Kul'chyns'kyi AB, Korolyshyn TA, Zukow W. Interrelations between changes in parameters of HRV, EEG and cellular immunity at patients with chronic pyelonephritis and cholecystitis. Journal of Education, Health and Sport. 2017; 7(10): 11-23.

55. Popovych IL, Babelyuk VY, Dubkova HI, Korolyshyn TA, Zukow W. Relationships between changes in parameters of manual function and electroencephalogram, heart rate variability as well as gas discharge visualization in children with spastic form of cerebral palsy caused by Kozyavkin© method. Experimental and Clinical Physiology and Biochemistry. 2018; 1(81): 39-50.
56. Popovych IL, Kul'chyns'kyi AB**,** Gozhenko AI, Zukow W, Kovbasnyuk MM, Korolyshyn TA**.** Interrelations between changes in parameters of HRV, EEG and phagocytosis at patients with chronic pyelonephritis and cholecystitis. Journal of Education, Health and Sport. 2018; 8(2): 135-156.
57. Popovych IL, Gozhenko AI, Zukow W, Polovynko IS. Variety of Immune Responses to Chronic Stress and their Neuro-Endocrine Accompaniment. Scholars' Press. Riga; 2020: 172 p.
58. Prinsloo GE, Rauch HG, Karpul D, Derman WE. The effect of a Single Session of Short Duration Heart Rate Variability Biofeedback on EEG: A Pilot Study. Appl Psychophysiol Biofeedback. 2013; 38(1): 45-56.
59. Romodanov AP (editor). Postradiation Encephalopathy. Experimental Researches and Clinical Observations [in Ukrainian and Russian]. Kyiv: USRI of Neurosurgery. 1993. 224 p.
60. Puchko LG. Multidimensional Medicine. Systen of Self-diagnosis and Self-healing of Human [in Russian]. 10th ed., rev. and ext. Moskva: ANS, 2004. 432 p.
61. Shakhbazov VG, Kolupaeva TV, Shuvalov IM et al. Method of rapid testing efficiency rehabilitation of health. Pat. 28113, Ukraine, NSI A61V10/00. 2000; Bul №5.
62. Shannon CE. Works on the theory of informatics and cybernetics [transl. from English to Russian]. Moskva. Inostrannaya literatura; 1963: 329 p.
63. Staats P, Giannakopoulos G, Blake J, Liebler E, Levy RM. The use of non-invasive vagus nerve stimulation to treat respiratory symptoms associated with COVID-19: A theoretical hypothesis and early clinical experience. Neuromodulation. 2020; 12: 10.1111/ner. 13172.
64. Sternberg EM. Neural regulation of innate immunity: a coordinated nonspecific response to pathogens. Nat Rev Immunol. 2006; 6(4): 318-328.
65. Subhani AR, Likun X, Saeed Malik A. Assotiation of autonomic nervous system and EEG scalp potential during playing 2D Grand Turismo 5. Conf Proc IEEE Eng Med Biol Soc. 2012: 3420-3423.
66. Tang Yi-Yuan, Ma Yinghua, Fan Yaxin et al. Central and autonomic nervous system interaction is altered by short-term meditation. Proc Natl Acad Sci USA. 2009; 106(22): 8865-8870.
67. Tolkunov D, Rubin D, Mujica-Parodi LR. Power spectrum scale invariance quantifies limbic dysregulation in trait anxious adults using fMRI: adapting methods optimized for characterizing autonomic dysregulation to neural dynamic timeseries. Neuroimage. 2010; 50(1): 72-82.
68. Tornero C, Vallejo R, Cedeño D, Orduña J, Pastor E, Belaouchi M, Escamila B, Laredo M, Garzando MM. A prospective, randomized, controlled study assessing vagus nerve stimulation using the gamma-Core®-Sapphire device for patient with moderate to severe CoViD-19 Respiratory Symptoms (SAVIOR): A structured summary of a study protocol for a randomized controlled trial. Trials. 2020; 21: 576.
69. Thayer JF, Sternberg EM. Neural aspects of immunomodulation: Focus on the vagus nerve. Brain Behav Immun. 2010; 24(8): 1223-1228.
70. Tracey KJ. Physiology and immunology of the cholinergic antiinflammatory pathway. J Clin Invest. 2007; 117(2): 289-296.
71. Tracey KJ. Understanding immunity requires more than immunology. Nature Immunology. 2010; 11(7): 561-564.
72. Vanneste S, De Ridder D. Brain Areas Controlling Heart Rate Variability in Tinnitus and Tinnitus-Related Distress. PloS ONE. 2013; 8(3): e59728.
73. Winkelmann T, Thayer JF, Pohlak ST, Nees F, Grimm O, Flor H. Structural brain correlates of heart rate variability in healthy young adult population. Brain Structure and Function. 2017; 222(2): 1061-1068.
74. Yoo HJ, Thayer JF, Greenig S, Lee TH,, Ponzio A, Min J, Sakaki M, Nga L, Mater M, Koenig J. Brain structural concomitants of resting state heart rate variability in the young and old: evidence from two independent samples. Brain Structure and Function. 2018; 223(2): 727-737.